CANCER BIOTHERAPY AND RADIOPHARMACEUTICALS
Volume 27, Number 10, 2012

DOI: 10.1089/cbr.2012.1225

Comparison of Cell-Labeling Methods with ^{124}I-FIAU and ^{64}Cu-PTSM for Cell Tracking Using Chronic Myelogenous Leukemia Cells Expressing HSV1-tk and Firefly Luciferase

Jae-Jun Park,[1] Tae-Sup Lee,[1] Jin-Ju Son,[1] Kwon-Soo Chun,[1] In-Ho Song,[1,2] Yong-Serk Park,[2] Kwang-Il Kim,[1] Yong-Jin Lee,[1] and Joo-Hyun Kang[1]

Abstract

Cell-tracking methods with molecular-imaging modality can monitor the biodistribution of cells. In this study, the direct-labeling method with ^{64}Cu-pyruvaldehyde-bis(N4-methylthiosemicarbazone) (^{64}Cu-PTSM), indirect cell-labeling methods with herpes simplex virus type 1-thymidine kinase (HSV1-tk)-mediated ^{124}I-2′-fluoro-2′-deoxy-1-β-D-arabinofuranosyl-5-iodouracil (^{124}I-FIAU) were comparatively investigated *in vitro* and *in vivo* for tracking of human chronic myelogenous leukemia cells. K562-TL was established by retroviral transduction of the *HSV1-tk* and *firefly luciferase* gene in the K562 cell. K562-TL cells were labeled with ^{64}Cu-PTSM or ^{124}I-FIAU. Cell labeling efficiency, viability, and radiolabels retention were compared *in vitro*. The biodistribution of radiolabeled K562-TL cells with each radiolabel and small-animal positron emission tomography imaging were performed. Additionally, *in vivo* and *ex vivo* bioluminescence imaging (BLI) and tissue reverse transcriptase–polymerase chain reaction (RT-PCR) analysis were used for confirming those results. K562-TL cells were efficiently labeled with both radiolabels. The radiolabel retention (%) of ^{124}I-FIAU (95.2% ± 1.1%) was fourfold higher than ^{64}Cu-PTSM (23.6% ± 0.7%) at 24 hours postlabeling. Viability of radiolabeled cells was statistically nonsignificant between ^{124}I-FIAU and ^{64}Cu-PTSM. The radioactivity of each radiolabeled cells was predominantly accumulated in the lungs and liver at 2 hours. Both the radioactivity of ^{64}Cu-PTSM- and ^{124}I-FIAU-labeled cells was highly accumulated in the liver at 24 hours. However, the radioactivity of ^{124}I-FIAU-labeled cells was markedly decreased from the body at 24 hours. The K562-TL cells were dominantly localized in the lungs and liver, which also verified by BLI and RT-PCR analysis at 2 and 24 hours postinjection. The ^{64}Cu-PTSM-labeled cell-tracking method is more efficient than ^{124}I-FIAU-labeled cell tracking, because of markedly decrease of radioactivity and fast efflux of ^{124}I-FIAU *in vivo*. In spite of a high labeling yield and radiolabel retention of ^{124}I-FIAU *in vitro*, the *in vivo* cell-tracking method using ^{64}Cu-PTSM could be a useful method to evaluate the distribution and targeting of various cell types, especially, stem cells and immune cells.

Key words: gene transfer, molecular imaging, PET

Introduction

The noninvasive monitoring of the transplanted cells and the tracking of their migration can facilitate basic research on the underlying mechanism and improve clinical translation of cell therapeutics. Conventional methods that employ tissue and blood sampling for tracking an injected cell population can be restricted to know the temporal information in living subject because of invasive research methods. Molecular imaging permits the temporal biodistribution of cells

[1]Molecular Imaging Research Center, Korea Institute of Radiological and Medical Sciences (KIRAMS), Seoul, Republic of Korea.
[2]Department of Biomedical Laboratory Science, Yonsei University, Wonju, Republic of Korea.

Address correspondence to: Tae-Sup Lee; Molecular Imaging Research Center, Korea Institute of Radiological and Medical Sciences (KIRAMS); 215-4 Gongneung-Dong, Nowon-Gu, Seoul 139-706, Republic of Korea
E-mail: **nobelcow@kirams.re.kr**

and related biological processes to be determined in a more meaningful manner throughout intact living subjects.[1–3]

The molecular-imaging modalities have been used for tracking of labeled cells with a magnetic probe,[4] a fluorescent probe,[5] bioluminescence imaging (BLI),[6–9] or a radiotracer[10–13] in *in vivo*. Among these methods, imaging techniques using radiotracers have the highest sensitivity and are mostly quantitative. Scintigraphy is a standard nuclear medicine approach and clinically established to characterize lesions.[14] Molecular-imaging strategies in the cell level require the tagging of the targets specifically expressed by individual cell populations. The assessment of cell trafficking can be pursued using *ex vivo* labeling; these cell labeling can be classified as either direct or indirect.[15] In direct cell labeling, a marker with no capacity for regeneration is introduced into the cell, usually by coincubation *in vitro*. Indirect cell labeling marks a cell with a reporter gene that is retained in subsequent regenerations. Reporter gene-based imaging methods permit the stable marking of the individual cell population with excellent sensitivity of detection. This approach is fundamental for imaging proliferating cell populations during their migration, activation, and division.

Scintigraphy imaging of cell tracking using positron emission tomography (PET) and single photon emission computed tomography (SPECT) have been extensively investigated and validated.[2] ^{111}In ($t_{1/2}$ = 68.2 hours)- and ^{99m}Tc ($t_{1/2}$ = 6.01 hours)-labeled T-lymphocyte, scintigraphy imaging has been widely used in clinical investigation.[14,16] However, radionuclides that decay with γ-energies lower than 100 keV produce too much scatter, while γ-energies over 250 keV are difficult to collimate, and therefore has a limitation for quantitative γ-scintigraphy. To overcome the disadvantages of γ-scintigraphy, the PET camera is designed to capture 511 keV photons emitted in an opposite direction and provide a better resolution and counting efficiency as compared to γ-scintigraphy and SPECT cameras.[17] However, a major limitation of PET imaging is the half-lives of the routinely used PET radionuclides, such as ^{18}F ($t_{1/2}$ = 1.8 hours). The use of longer lived positron emitters is able to long-term tracking of transplanted cells. As compared to ^{18}F, ^{64}Cu has a longer half-life of 12.7 hours and a similar β^+ yield (0.66 MeV). The image quality and spatial resolution (0.70 mm) are equivalent to ^{18}F. Those characteristics make ^{64}Cu an attractive radionuclide for PET imaging. Recently, the feasibility of labeling cells with ^{64}Cu-pyruvaldehyde-bis(N4-methylthiosemicarbazone) (^{64}Cu-PTSM) or ^{64}Cu-labeled polyethylenimine has been evaluated and the tracking of labeled cells was successfully visualized by PET.[10,11]

Iodine-124 ($t_{1/2}$ = 4.08 days) is a positron-emitting radionuclide with high-energy γ-emissions (0.6 MeV, 61%) and high-energy positron emissions (2.14 MeV, 24%). The spatial resolution of ^{124}I (3.25 mm) is poor, but the relatively longer half-life makes ^{124}I conductive for indirect labeling of cells for PET imaging.[17] Koehne and colleagues have reported the strategy for *in vivo* imaging of tumor-targeting T lymphocytes that are radiolabeled with ^{124}I-FIAU or ^{131}I-FIAU *in vivo* as early as 24 hours after i.v. injection.[12,13]

Both direct and indirect labeling are useful methods for *in vivo* cell tracking, nevertheless, their advantage or disadvantage has not yet been comparatively investigated. In this study, we compared the *in vitro* labeling efficiency, label retenition, and cell viability of human chronic myelogenous leukemia cells containing the herpes simplex virus type 1-thymidine kinase (*HSV1-tk)* and the firefly luciferase gene. Direct-labeled cells using ^{64}Cu-PTSM and indirect-labeled cells using ^{124}I-2′-fluoro-2′-deoxy-1-β-D-arabinofuranosyl-5-iodouracil (^{124}I-FIAU) were comparatively investigated by using the small-animal PET and biodistribution study. Bioluminescence monitoring and reverse transcriptase–polymerase chain reaction (RT-PCR) analysis were also used for evaluating *in vivo* distribution of cells.

Materials and Methods

Cell culture

K562, the human chronic myelogenous leukemia cell line was purchased from American Type Culture Collection. K562 cells were grown in RPMI 1640 supplemented with 10% fetal bovine serum (FBS) and antibiotics/antimycotics (Gibco BRL).

Retroviral transfer of HSV1-tk *and* firefly luciferase *gene*

Gene transfer was performed with the MFG retroviral vector system.[18] Briefly, the retroviral vector employ the moloney murine leukemia virus long terminal repeat sequences for the expression of inserted *HSV1-tk* gene and harbors a CMV promoter-driven *firefly luciferase* gene. The resulting vector constructs were introduced into H29D cells to generate recombinant virus with amphotropic host range. K562 cells were transduced in the presence of 0.8 μg/mL polybrene (Sigma). The transfected K562 cells were plated on a 96-well plate as one cell per a well. These stably transfected cells were selected by a luminometer and termed K562-TL cells.

Cell labeling with ^{124}I-FIAU

Radioiodinated FIAU was prepared as previously described.[19] Carrier-free synthesis of radioiodinated FIAU was performed with a stannylated precursor, 5-tributylstannyl-1-(2′-deoxy-2′-fluoro-β-D-arabino-furanosyl)uracil, which was allowed to react with Na^{124}I (MC-50 cyclotron; Korea Institute of Radiological and Medical Sciences [KIRAMS]) in the presence of a mixture of acetic acid and 30% hydrogen peroxide. After quenching with sodium metabisulfite, the radioiodinated FIAU was isolated on a C-18 Sep-Pak cartridge (Waters), and eluted with ethanol. The ethanol was evaporated and the radioiodinated FIAU was formulated with a cell culture medium or saline. The radiochemical purity was measured by radio-high-performance liquid chromatography (HPLC). HPLC was performed by previously described methods.[20] Radiolabeled FIAU with a fixed amount of radioactivity (3.7 MBq/0.1 mL) was treated to 5×10^6 of K562-TL cells in a total volume of 10 mL at 37°C for 4 hours. The cell-bound radioactivity was measured by the gamma counter 1480 WIZARD (Perkin-Elmer).

Cell labeling with ^{64}Cu-PTSM

^{64}Cu was produced at KIRAMS by 50 MeV cyclotron irradiation using methods reported.[21] PTSM was purchased from ABX. ^{64}Cu-PTSM was prepared by minor modifications of previous methods.[10] In brief, a 10 μL of PTSM (1 mg/mL

in dimethyl sulfoxide) was added to 150 μL of ^{64}Cu-acetate solution, which $^{64}CuCl_2$ diluted with 1 M sodium acetate, pH 5.5 and vortexed briefly. After 3–5 minutes, the mixture was added to an ethanol-preconditioned C-18 Sep-Pak cartridge. ^{64}Cu-PTSM was eluted off with 500 μL of ethanol after removal of the initial 150-μL fraction. The radioactive fraction was checked for radiochemical purity by silica gel thin layer chromatography using ethyl acetate as a mobile phase. ^{64}Cu-PTSM (3.7 MBq) was incubated with K562-TL cells (5×10^6) with the RPMI 1640 medium containing 5% FBS and 5% ethanol in a total volume of 10 mL at 37°C for 4 hours. After twice washing with phosphate-buffered saline at each incubation time, the pellets were counted using the gamma counter.

In vitro *stability and viability of radiolabeled K562-TL cells*

Evaluation of radiolabels stability and cell viability has been previously described.[13] The radioactivity retention (%) of the radiolabels in the K562-TL was assessed by incubating radiolabeled K562-TL cells with the fresh RPMI 1640 medium for 1, 3, 6, and 24 hours. The radioactivity of cells was counted in a gamma counter. Viability of radiolabeled K562-TL cells was measured by 0.4% trypan blue dye exclusion in a Neubauer hemocytometer. The viabilities were expressed as percentage of viable cells among the total number of cells.

Biodistribution of radiolabeled K562-TL cells

For evaluating the biodistribution of radiolabeled K562-TL cells, K562-TL cells labeled with ^{124}I-FIAU (370 KBq/5×10^6 cells/head, $n=4$), or ^{64}Cu-PTSM (740 KBq/5×10^6 cells/head, $n=4$) were administered into the tail vein. Athymic female BALB/c mice (18–20 g body weight) were obtained from Japan SLC and were handled in accordance with the institutional guidelines of the KIRAMS. At 2 and 24 hours postinjection, the mice were sacrificed and the blood and various tissues were collected, weighed, and measured for radioactivity in a gamma counter. The radioactivity of tissues was expressed as percentage of the injected radioactivity dose per gram of tissue (%ID/g) or percentage of the injected activity per tissue (%ID) per tissue.

Small-animal PET imaging

PET studies were performed using a small-animal dedicated PET scanner (microPET-R4; Concorde Microsystems). Mice ($n=2$/group) were injected through the tail vein with ^{64}Cu-PTSM (629 KBq/0.1 mL), ^{64}Cu-PTSM-labeled K562-TL cells (480 KBq/5×10^6 cells/0.2 mL), or ^{124}I-FIAU-labeled K562-TL cells (740 KBq/5×10^6 cells/0.2 mL). The mice injected with ^{64}Cu-PTSM were used as control. The small-animal PET images were acquired at 10 minutes, 2, 13.5, and 23 hours postinjection of ^{64}Cu-PTSM and at 10 minutes, 2, 12, and 23 hours postinjection of ^{64}Cu-PTSM and ^{124}I-FIAU-labeled K562-TL cells. The mice were scanned for 60 minutes static image. All mice were scanned in a prone position. The digital whole-body autoradiography immediately performed after 23 hours scan. The acquired 3D emission list-mode data were reconstructed to image using Fourier rebining and ordered subsets expectation maximization reconstruction algorithm without attenuation corrections.[22] Image visualization was performed using the ASIPro (microPET®; Concorde Microsystems) display software.

Digital whole-body autoradiography

Immediately after PET scanning, mice were sacrificed by a high-dose intraperitoneal injection of ketamine and xylazine, and the digital whole-body autoradiography was performed by previously described methods with minor modifications.[23] In brief, sacrificed mice were transferred and frozen at −70°C deep freezer. Coronal whole-body mouse sections (30-μm thick) were obtained by whole-body autocryotome (Nakagawa Seisakusho), the frozen sections were exposed to an image plate for 24ioours, and the plates were scanned with BAS-5000 (Fujifilm). An autoradiogram and its corresponding photo section were shown to the adjacent of the small-animal PET image to link the radioactive signal with anatomy.

Bioluminescence imaging

BLI was performed with IVIS-200 imaging system (Calipers). Imaging and quantification of bioluminescent signals were acquired and analyzed with Living Image 2.50 software. The expression of the *firefly luciferase* gene in K562-TL cells was verified by using the Bright-Glo kit (Promega) and the correlation between the bioluminescent signal intensity and the K562-TL cell number was also checked. Mice were injected intravenously with 5×10^6 K562-TL cells for *in vivo* and *ex vivo* BLI. The same mice received an intraperitoneal injection of 125ere injɒ-luciferin for *in vivo* BLI or 500 or trapɒ-luciferin for *ex vivo* BLI (Molecular Imaging Products Company) and anesthetized with 2.5% isoflurane in 100% O_2 condition. Mice were placed and acquired in a ventral view for 5 werutes at 5 vieutes postinjection of luciferin. After *in vivo* BLI, the liver, lungs, spleen, and blood were excised for RT-PCR analysis. For *ex vivo* BLI, mice were sacrificed and various tissues were obtained and imaged for 5 minutes. The bioluminescent signal intensity represents as photons/seconds.

RT-PCR analysis

Total RNA was prepared from K562, K562-TL cells, and various tissues of K562-TL cells injected mice using the Easy-spin™ (iNtRON Biotechnology) or Trizol Reagent (MRC). RT-PCR was performed with forward and reverse primers of the *HSV1-tk* (5′-ctc acc ctc atc ttc gac cg-3′cand 5′-cct gca gat acc gca ccg ta-3′) using the GeneAmp PCR system 9700 (Applied Biosystems). β-actin (5′-ata tcg cgc tgg tcg tc-3′ and 5′-agg atg gcg tga ggg aga gc-3′) or GAPDH (5′-agg ccg gtg ctg agt atg tc-3′ and 5′-tgc ctg ctt cac cac ctt ct-3′) was amplified as a control. The amplified products were analyzed by ethidium bromide stained agarose gel electrophoresis. The amount of each fragment was determined with a densitometer.

Western blot analysis

Sodium dodecyl sulfate–polyacrylamide gel electrophoresis (SDS-PAGE) was carried out on 10% polyacrylamide gels by the method of Laemmli[24] Total protein was extracted from K562 and K562-TL cells and analyzed by SDS-PAGE. The gel was electroblotted onto polyvinylidene fluoride

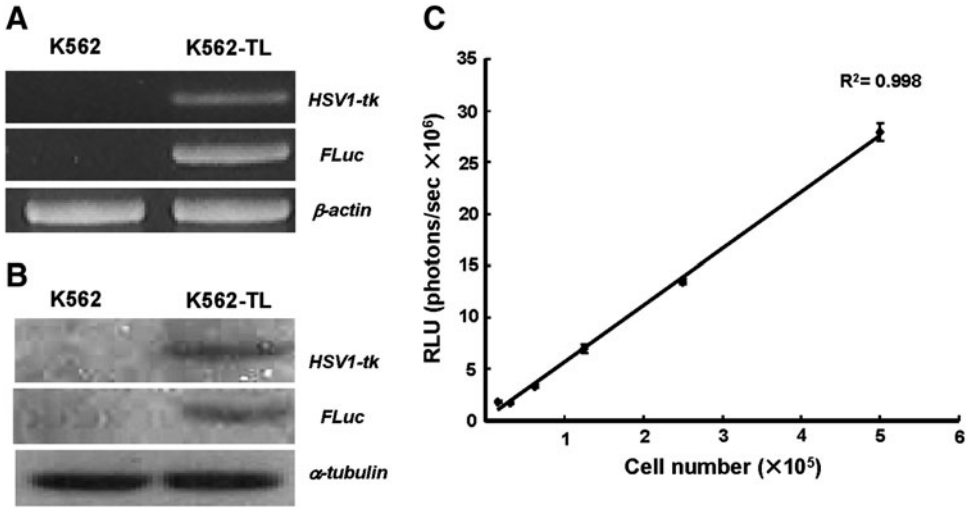

FIG. 1. Establishment of HSV1-tk and firefly luciferase expressing K562 cell line (K562-TL). The human chronic myelogenous leukemia cell line, K562-TL expressed HSV1-tk and firefly luciferase **(A)** in mRNA level by RT-PCR and **(B)** protein level by Western blot. **(C)** K562-TL cell number was well correlated with bioluminescent signal intensity ($R^2 = 0.998$). HSV1-tk, herpes simplex virus type 1-thymidine kinase; RT-PCR, reverse transcriptase–polymerase chain reaction.

membranes (Bio-Rad). Immunoblot analysis was carried out using the anti-HSV1-tk polyclonal antibody (kindly provided by Dr. W. Summers, Yale University), antiluciferase polyclonal (Promega), and anti-α-tubulin monoclonal (Sigma) antibodies. Peroxidase anti-mouse and goat antibodies (Sigma) were used for the secondary antibody. Detection was performed using an ECL Western blot detection kit (Amersham Bioscience).

Statistical analysis

Quantitative data were expressed as mean ± standard deviation. Means were compared using the Student's *t*-test. p Values < 0.05 were considered statistically significant.

Results

Establishment of HSV1-tk and firefly luciferase-expressing K562 cells

Stable transduction of the *HSV1-tk* and *firefly luciferase* gene was confirmed by RT-PCR analysis (Fig. 1A). The primers for viral thymidine kinase gene and luciferase gene sequence yielded amplification products of the expected size 281 and 400 bp, respectively. To verify that the protein was stably expressed in the transduced cell line, the expression of HSV1-TK and luciferase were checked by immunoblot. The bands of correct size for HSV1-TK (47 kDa) and luciferase (62 kDa) were detected in K562-TL cells, but not in control K562 cells (Fig. 1B). To assess the relationship between bioluminescent signal intensities and viable cell numbers, we prepared a serial dilution of the K562-TL cells (1.6×10^5–5.0×10^6 cells/well) and measured the bioluminescent signals. The bioluminescent intensity increased in proportion to the increasing cell numbers and the relative luminescent signals per cell was constant (5.11–5.93 photons/seconds per cell) (Fig. 1C).

In vitro *cell labeling*

The radiochemical yield of ^{124}I-FIAU and ^{64}Cu-PTSM was 54.3% ± 11.3% and 86.0% ± 5.7%, respectively. The HPLC and thin layer chromatography analysis of each radiotracer indicated that radiochemical purity is above 98%. The labeling efficiency in K562-TL cells was evaluated to determine the optimal labeling condition for *in vivo* studies. The time-dependent uptake of ^{124}I-FIAU and ^{64}Cu-PTSM in K562-TL cells is shown as cell-bound radioactivity (Fig. 2). The results indicate that ^{124}I-FIAU and ^{64}Cu-PTSM was rapidly accumulated into cells for 1 hour, thereafter ^{64}Cu-PTSM reached the saturation level between 120 and 240 minutes. The labeling efficiency of K562-TL cells with ^{124}I-FIAU was 26.3% ± 1.6% and 32.5% ± 1.1% at 120 and 240 minutes, respectively. With ^{64}Cu-PTSM, the labeling efficiency was 16.4% ± 1.2% and 18.2% ± 2.1% at 120 and 240 minutes, respectively. We determined the optimal incubation time of ^{124}I-FIAU and ^{64}Cu-PTSM was 240 minutes.

The cell viability and efflux of radiolabels

The viability of K562-TL cells was evaluated during and after radiolabeling (Fig. 3A). As measured by the trypan blue dye exclusion test, K562-TL cells labeled with ^{64}Cu-PTSM for

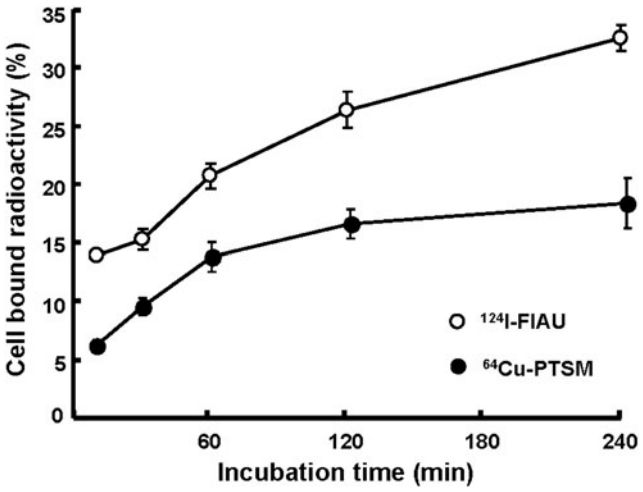

FIG. 2. *In vitro* cellular uptakes of ^{124}I-FIAU and ^{64}Cu-PTSM in K562-TL cells. Radiotracer uptakes were increased as time-dependent manners. ^{124}I-FIAU, ^{124}I-2′-fluoro-2′-deoxy-1-β-D-arabinofuranosyl-5-iodouracil; ^{64}Cu-PTSM, ^{64}Cu-pyruvaldehyde-bis(N4-methylthiosemicarbazone).

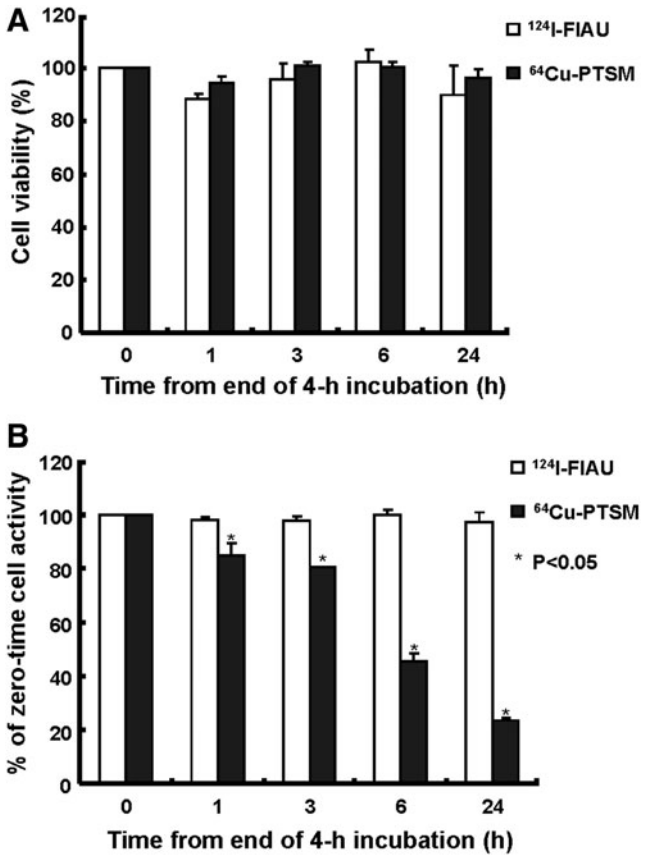

FIG. 3. The viability and radioactivity retention of ^{124}I-FIAU- and ^{64}Cu-PTSM-labeled K562-TL cells. **(A)** Cell viability (%) of radiotracer-labeled cells was not significantly changed. **(B)** Relative cell-bound radioactivity (%) of K562-TL cells labeled with ^{124}I-FIAU and ^{64}Cu-PTSM during incubation in a tracer-free medium.

240 minutes showed approximately 80% viability, because of the use of ethanol during incubation with ^{64}Cu-PTSM. However, there was no significant difference in viability of cells labeled with ^{124}I-FIAU for 240 minutes (data not shown). At 24 hours postradiolabeling, the viability of K562-TL cells with ^{124}I-FIAU and ^{64}Cu-PTSM was 89.9%±11.4% and 96.3%±3.5%, respectively (Fig. 3A). There was little effect on the cell viability ($p>0.1$) for 24 hours after ^{64}Cu-PTSM and ^{124}I-FIAU uptake in K562-TL cells. To evaluate the efflux of ^{124}I-FIAU and ^{64}Cu-PTSM, the retained radioactivity of labeled K562-TL cells was measured (Fig. 3B). ^{64}Cu-PTSM was rapidly released from K562-TL cells, with average decreases of 15.5% of initial cell-bound activity after 1 hour and 54.4% of that after 6 hours. As shown in Figure 3B, following a slightly decrease of ^{124}I-FIAU radioactivity by 1 hour, there was no significant change of radioactivity up to 24 hours. However, a significant loss of ^{64}Cu-PTSM was detected by 76.4% up to 24 hours.

Biodistribution of radiolabeled K562-TL cells

The biodistribution of ^{124}I-FIAU- and ^{64}Cu-PTSM-labeled cells was determined at 2 and 24 hours postinjection (Tables 1 and 2). The highest radioactivity of the ^{124}I-FIAU-labeled cell was found in the lungs (39.51±10.93%ID/g) at 2 hours. At this time, the radioactivity in the liver reached 7.71±1.72%ID/g, and thereafter radioactivity of the lungs and liver decreased to 0.09±0.02%ID/g and 0.04±0.01%ID/g, respectively, at 24 hours postinjection. In ^{64}Cu-PTSM-labeled cell-injected mice, the lungs showed highest radioactivity as 29.25±3.31%ID/g and the radioactivity of liver was 11.90±0.89%ID/g at 2 hours. And then that radioactivity decreased to 7.25±1.17%ID/g and 4.25±0.78%ID/g, respectively, at 24 hours (Table 1).

The biodistribution of radiolabeled K562-TL cells was also presented as a %ID(Table 2). The liver showed a high radioactivity in both ^{124}I-FIAU- and ^{64}Cu-PTSM-labeled K562-TL cells at 2 hours postinjection. At this time, the activity in the liver was 7.13±1.62%ID for ^{124}I-FIAU-labeled cells and 12.57±0.82%ID for ^{64}Cu-PTSM-labeled cells. ^{64}Cu-PTSM accumulation in the liver remained high level for 24 hours postinjection (8.10±0.74%ID). Compared to the ^{64}Cu-PTSM-labeled cell-injected group at 24 hours, the radioactivity of ^{124}I-FIAU-labeled cells was significantly decreased in all major organs except thyroid (1.229±0.264%ID) and small intestine (0.337±0.090%ID). Thyroid uptake of free iodine

Table 1. Biodistribution (%ID/g) of Radiolabeled K62-TL Cells in BALB/c Nude Mice

	^{64}Cu-PTSM		*^{124}I-FIAU*	
Tissue	*2 hours*	*24 hours*	*2 hours*	*24 hours*
Blood	0.77±0.11	1.01±0.14	5.20±1.60	0.04±0.01
Heart	1.63±0.08	2.78±0.25	2.65±0.88	0.03±0.01
Liver	11.90±0.89	7.25±1.17	7.71±1.72	0.04±0.01
Lung	29.25±3.31	4.25±0.78	39.51±10.93	0.09±0.02
Spleen	8.50±1.61	3.14±0.41	3.46±0.79	0.17±0.08
Kidney	5.24±0.51	4.36±0.63	5.62±0.96	0.05±0.01
Stomach	1.23±0.35	1.19±0.30	9.99±4.32	0.25±0.07
Small intestine	4.17±0.56	2.15±0.38	2.63±0.51	0.30±0.08
Large intestine	4.98±0.79	3.79±0.63	5.47±1.34	0.15±0.00
Thyroid	1.62±0.85	0.07±0.02	1.28±0.58	1.32±0.23
Muscle	0.40±0.06	0.58±0.07	1.57±0.48	0.04±0.02
Femur	0.85±0.08	1.00±0.17	1.90±0.38	0.25±0.11

All the values are given as a percentage of the injected activity per gram of tissue.
Data are presented as mean±SD for 4 animals.
%ID/g, percentage of the injected radioactivity dose per gram of tissue; ^{64}Cu-PTSM, ^{64}Cu-pyruvaldehyde-bis(N4-methylthiosemicarbazone); ^{124}I-FIAU, ^{124}I-2′-fluoro-2′-deoxy-1-β-D-arabinofuranosyl-5-iodouracil; SD, standard deviation.

Table 2. Biodistribution (%ID) of Radiolabeled K562-TL Cells in BALB/c Nude Mice

	^{64}Cu-PTSM		^{124}I-FIAU	
Tissue	*2 hours*	*24 hours*	*2 hours*	*24 hours*[a]
Heart	0.18 ± 0.01	0.27 ± 0.03	0.27 ± 0.08	0.004 ± 0.001
Liver	12.57 ± 0.82	8.10 ± 0.74	7.13 ± 1.62	0.051 ± 0.007
Lung	3.47 ± 0.32	0.56 ± 0.11	5.31 ± 2.42	0.022 ± 0.019
Spleen	0.44 ± 0.09	0.25 ± 0.06	0.25 ± 0.03	0.022 ± 0.010
Kidney	1.40 ± 0.11	1.25 ± 0.11	1.42 ± 0.31	0.014 ± 0.002
Stomach	0.50 ± 0.02	0.32 ± 0.04	5.27 ± 1.42	0.050 ± 0.005
Small intestine	5.24 ± 0.92	2.25 ± 0.31	3.02 ± 0.46	0.337 ± 0.090
Large intestine	3.88 ± 0.76	3.13 ± 0.62	3.32 ± 0.64	0.096 ± 0.019
Thyroid	0.07 ± 0.02	0.07 ± 0.01	1.18 ± 0.51	1.229 ± 0.264

All the values are given as a percentage of the injected activity per tissue.
Data are presented as mean ± SD for 4 animals.
[a]Data are presented as 10^{-3} order of mean ± SD for 4 animals, because of low radioactivity.
%ID, percentage of the injected activity per tissue.

from deiodinated FIAU was detected at 24 hours. Both ^{124}I-FIAU and ^{64}Cu-PTSM were mainly excreted through the gastrointestinal tract. At 24 hours, the radioactivity of ^{124}I-FIAU in the liver (0.051 ± 0.007%ID) is higher than other major organs except thyroid and intestines. The radioactivity uptake pattern in major organs did not differ between mice administered with ^{64}Cu-PTSM and ^{124}I-FIAU; however, uptakes (%ID) of ^{124}I-FIAU in various organs were significantly lower than those of ^{64}Cu-PTSM.

Small-animal PET imaging

The microPET scanner was used to image the distribution of radiolabeled K562-TL cells (Figs. 4–6). The anatomical position of radioactivity in the microPET deduced from whole-body frozen section photo. To verify the distribution of ^{64}Cu-PTSM-labeled K562-TL cells, ^{64}Cu-PTSM-injected mice were imaged as a control (Fig. 4). MicroPET images of mice injected with ^{64}Cu-PTSM showed primarily localization of radiotracer in the liver and heart from 10 minutes to 23 hours. Minimal radioactivity was detected in the lungs from 10 minutes to 23 hours in ^{64}Cu-PTSM-injected mice. ^{64}Cu-PTSM-labeled cells mainly localized in the lungs and liver at 2 hours postinjection (Fig. 5). The radioactivity was excreted through the intestine. Radioactivity in the lungs was markedly decreased and radioactivity in theliver retained for 23 hours. The microPET images were correlated with the biodistribution of ^{64}Cu-PTSM-labeled cells. As shown in Figure 6, radioactivity of ^{124}I-FIAU-labeled cells was mainly detected in the lungs and the liver at 2 hours postinjection. Although the radioactivity of thyroid and intestine remained until 24 hours postinjection, the entire radioactivity was significantly decreased in ^{124}I-FIAU-labeled cells injected mice. The radioactivity of liver was not visualized in

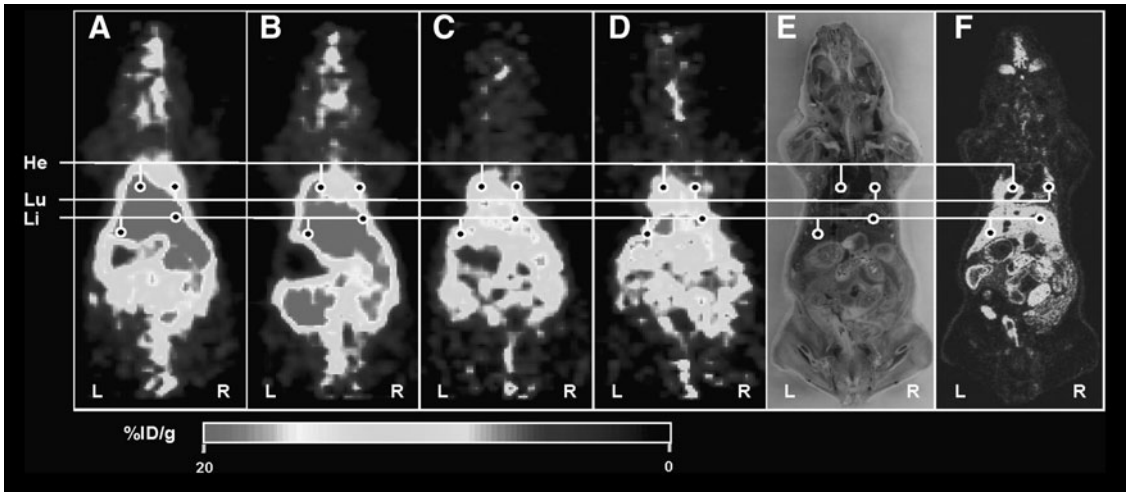

FIG. 4. Small-animal PET imaging of ^{64}Cu-PTSM. The PET images were obtained at 10 minutes **(A)**, 2 hours **(B)**, 12 hours **(C)**, and 24 hours **(D)** postinjection. **(E)** Photo of DWBA section shown in **(F)**. **(F)** DWBA image. At 10 minutes postinjection, liver is the primary targeting organ and heart represents the blood radioactivity of ^{64}Cu-PTSM **(A)**, but at 23 hours, the radioactivities were excreted through intestines **(D)**. The %ID/g represents the magnitude of radioactivity signal quantified in each small-animal PET image. He, heart; Lu, lung; Li, liver; PET, positron emission tomography; DWBA, digital whole-body autoradiography; %ID/g, percentage of the injected radioactivity dose per gram of tissue.

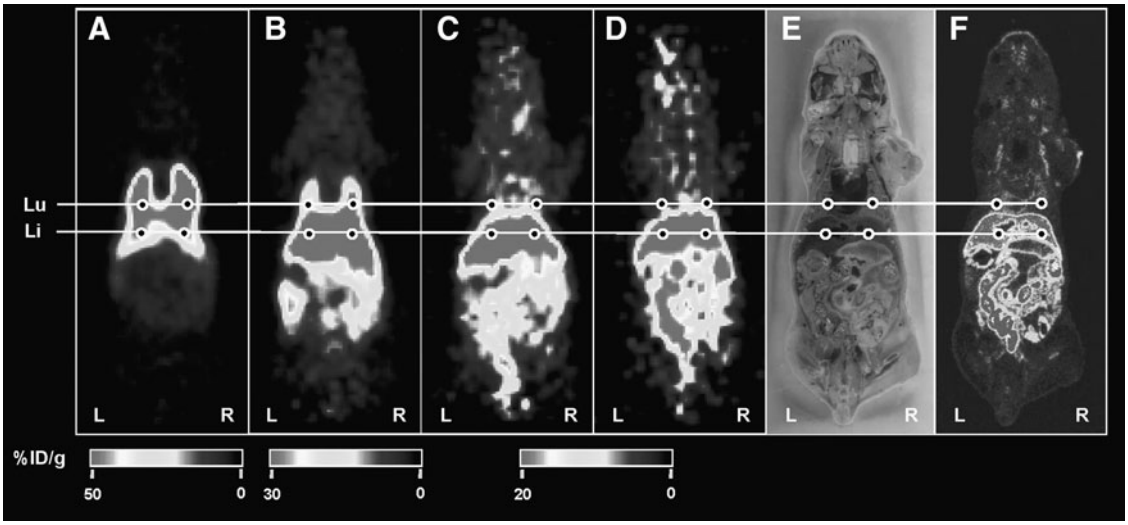

FIG. 5. Small-animal PET imaging of ^{64}Cu-PTSM-labeled K562-TL cells. The PET images were obtained at 10 minutes **(A)**, 2 hours **(B)**, 12 hours **(C)**, and 24 hours **(D)** postinjection. **(E)** Photo of DWBA section shown in **(F)**. **(F)** DWBA image. At 10 minutes postinjection, the lungs are the primary targeting sites **(A)**, but at 23 hours, the liver is major accumulation site **(D)** in ^{64}Cu-PTSM-labeled K562-TL cells injected mice. The %ID/g represents the magnitude of radioactivity signal quantified in each small-animal PET image. Lu, lung; Li, liver.

micro PET image at 24 hours postinjection. It may be caused by low radioactivity retention of ^{124}I-FIAU-labeled cells in the liver.

Bioluminescence monitoring of K562-TL cells

In vivo trafficking of K562-TL cells was confirmed with BLI by using firefly luciferase (Fig. 7A). The highest signal intensity was mainly detected in the lungs at 1 and 2 hours after the K562-TL cell injection. At 24 hours postinjection, weak bioluminescent signal intensities were measured in the liver and intestine region. The e*x vivo* bioluminescent signal (photons/seconds) was measured to quantitative bioluminescent intensity in various tissues (Fig. 7B). The quantification of *ex vivo* bioluminescence indicated that the bioluminescent signal intensity in the lungs (3.15×10^5 photons/seconds) was higher than that in any other organs at 2 hours postinjection. The overall bioluminescence intensity was low and the signal intensity of the liver (1.23×10^5 photons/seconds) and the large intestines (9.61×10^4 photons/seconds) was higher compared with other tissues at 24 hours postinjection. The bioluminescence intensity of other tissues was

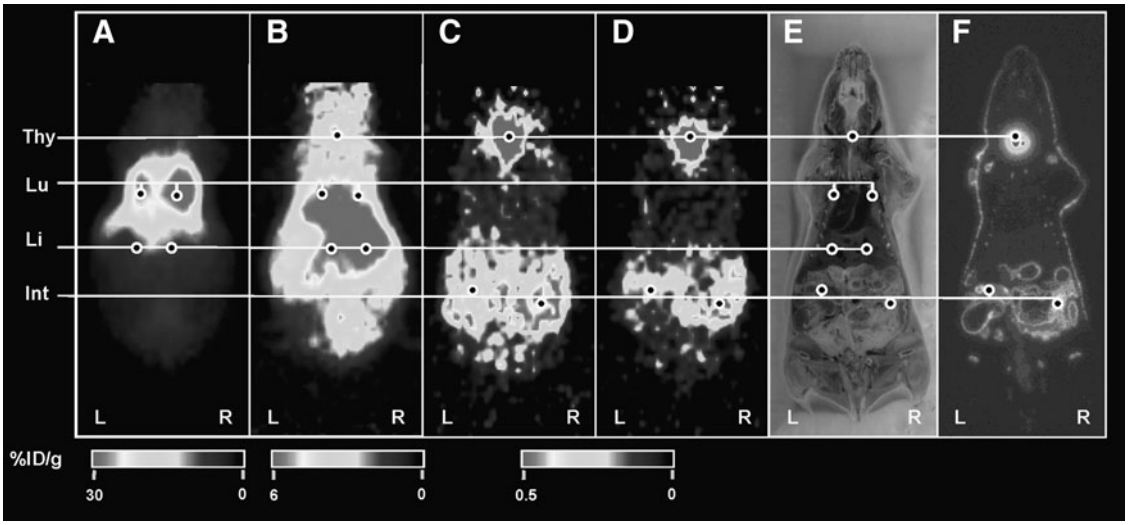

FIG. 6. Small-animal PET imaging of ^{124}I-FIAU-labeled K562-TL cells. The PET images were obtained at 10 minutes **(A)**, 2 hours **(B)**, 12 hours **(C)**, and 24 hours **(D)** postinjection. **(E)** Photo of DWBA section shown in **(F)**. **(F)** DWBA image. At 10 minutes postinjection, the lungs are the primary targeting sites **(A)**, but at 23 hours, the overall radioactivities were significantly decreased **(D)** in ^{124}I-FIAU-labeled K562-TL cells injected mice. The %ID/g represents the magnitude of radioactivity signal quantified in each small-animal PET image. Thy, thyroid; Lu, lung; Li, liver; Int, intestine.

nearly baseline levels at all time points. Those results showed a similar distribution pattern with biodistribution data of ^{64}Cu-PTSM- or ^{124}I-FIAU-labeled K562-TL cells.

RT-PCR analysis of in vivo distribution of K562-TL cells

The presence of K562-TL cells within the tissues was also determined by RT-PCR. HSV1-tk messenger RNA (mRNA) was found to be present within the blood, lungs, and liver at 2 hours postinjection (Fig. 8). Twenty-four hours after injection, HSV1-tk mRNA was detected in the blood, spleen, and liver. The mRNA expression level was represented as the ratio of the amount of HSV1-tk fragment over GAPDH. The expression of HSV1-tk mRNA (arbitrary unit) in both lungs (19.3) and blood (16.5) was significantly higher than that in the median lobe and the left lobe of liver (10.7 and 9.6, respectively), at 2 hours postinjection. The overall expression level of HSV1-tk in tissues was markedly decreased at 24 hours, compared to that at 2 hours. HSV1-tk mRNA was found in the left lobe of liver (8.3), blood (6.6), and spleen (6.0), but the transcript was not detected in the lungs at 24 hours postinjection. The expression ratio in various tissues was similar with the distribution pattern of *ex vivo* bioluminescence intensity of K562-TL cells and also confirmed biodistribution data of ^{64}Cu-PTSM- or ^{124}I-FIAU-labeled cells.

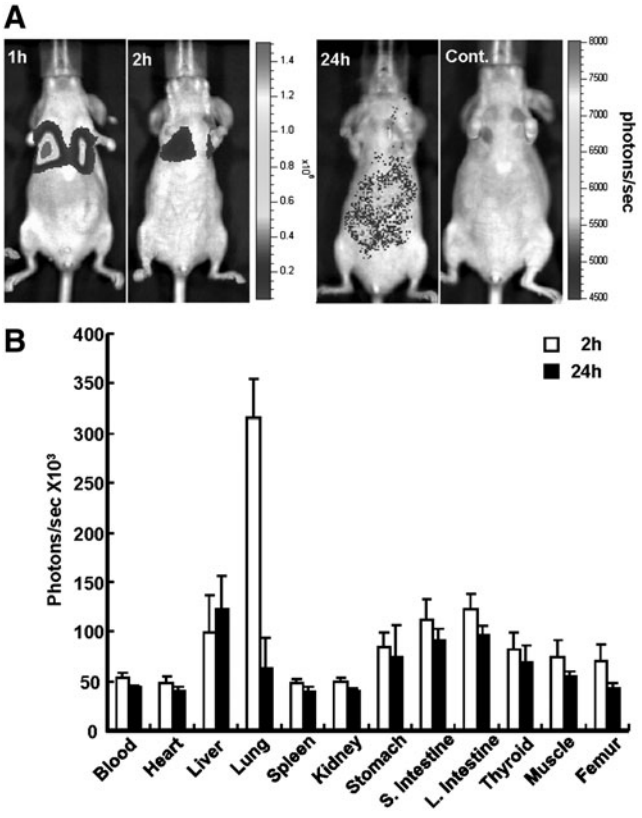

FIG. 7. Bioluminescence monitoring in K562-TL cells intravenously injected nude mice. **(A)** *In vivo* bioluminecence images of K562-TL cells at 1, 2, and 24 hours postinjection and control (noninjected mice). **(B)** *Ex vivo* bioluminescent signals of various tissues in K562-TL cells injected mice at 2 and 24 hours postinjection.

Discussion

In this study, direct-labeled cells using ^{64}Cu-PTSM and indirect-labeled cells using ^{124}I-FIAU were comparatively investigated *in vitro* and *in vivo*. ^{124}I-FIAU showed an *in vitro* higher radioactivity accumulation and a slower efflux than ^{64}Cu-PTSM in K562-TL cells. However, the cell-labeling method using HSV1-tk-mediated ^{124}I-FIAU uptake was not suitable for the *in vivo* cell-trafficking image using small-animal PET, because of its fast *in vivo* efflux at 24 hours. On the other hand, *in vivo* biodistribution of ^{64}Cu-PTSM-labeled cells showed a strong correlation with BLI and RT-PCR data. Overall, our results show that ^{64}Cu-PTSM is the most appropriate radiolabel for the noninvasive tracking of cells until 24 hours postinjection.

The use of HSV1-tk as a reporter gene is the most common technique for selective *in vivo* imaging.[12,23,25,26] Radiolabeled nucleoside analogues easily penetrate across the cell membrane. Therefore, tumor cells expressing HSV1-tk were selectively visualized by radiolabeled FIAU incorporation.[25,26] Koehne et al.[12] used ^{131}I-FIAU and target specific lymphocyte for cell tracking, which was based on *ex vivo* labeling with FIAU and reinfusion of labeled cells, which potentially allows more specific tracking of the cell labeled by the reporter gene. The radioactivity of intravenously injected *ex vivo* FIAU-labeled lymphocytes was accumulated in the liver and lungs at early time point (1 hours) and was too low to detect in the liver region at late time point (24 hours). These results correspond well with our study, which is that the ^{124}I-FIAU-labeled K562-TL cells demonstrate to be localized in the lungs and liver at 2 hours postinjection and the majority of injected radioactivity in the mice at 24 hours may be excreted by urine and the gastrointestinal tract.[12,27]

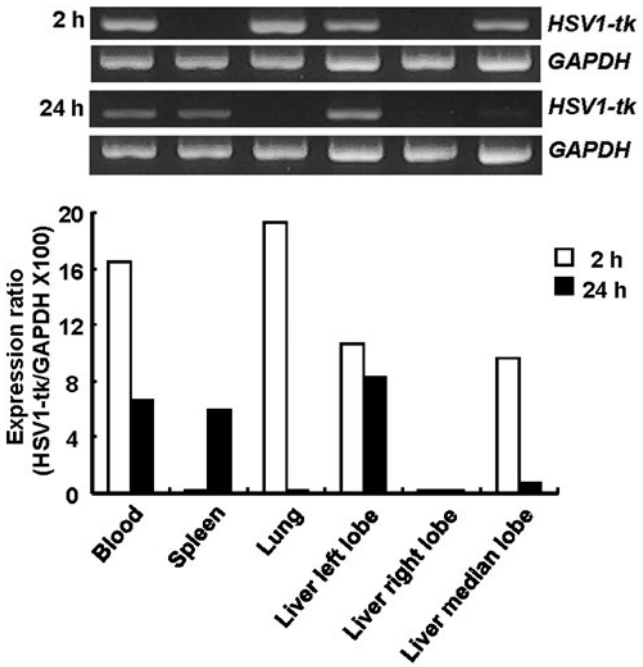

FIG. 8. RT-PCR analysis in K562-TL cells intravenously injected nude mice. HSV1-tk gene expression was confirmed using RT-PCR analysis in various tissues of K562-TL cells injected mice at 2 and 24 hours postinjection.

Haubner et al.[28] reported radiolabeled FIAU, which is released from labeled cells would be significantly cleared from mouse after cell injection. In blood, radiolabeled FIAU is almost resistant to metabolic degradation and 2'-fluoro in FIAU provides a protective group against enzymatic cleavage of the N-glycosidic bond by nucleoside phosphorylases.[29] In addition, studies by Chou et al.[30] on the metabolism of FIAU showed that most of the activity was found in the urine, clearly demonstrating the *in vivo* stability of this compound. In spite of its stability, the localization of radioactivity to thyroid at 24 hours indicates some deiodination of ^{124}I-FIAU *in vivo*.[28,31] The radioactivity of ^{124}I-FIAU in the liver (0.051 ± 0.007%ID) at 24 hours was higher than other organs except the thyroid and gastrointestinal tract. However, the radioactivity (%ID) of ^{124}I-FIAU in the liver was too low to visualize the biodistribution of radiolabeled K562-TL cells *in vivo* by using micro PET at 24 hours postinjection.

The direct cell-labeling techniques for *in vivo* monitoring of lymphocyte trafficking have been used radioactive probe such as ^{99m}Tc-hexamethylpropylene amine oxime or ^{111}In-oxine.[14,32,33] Recently, cell labeling with ^{64}Cu-PTSM was used for cell-trafficking approaches.[10,34] There are some features that make ^{64}Cu-PTSM an attractive radiotracer for the cell-trafficking study. First, in contrast to the short half-life of many β^+ emitters, its half-life of 12.7 hours is long enough for the cell-tracking study with PET. Second, imaging characteristics as a result of optimum positron energy (0.66 MeV) and no high energy of γ-emission make a high image quality and spatial resolution. Third, a lipophilic chelator, PTSM, can be used to transfer ^{64}Cu across the cell membrane efficiently. Because lipophilicity of the ^{64}Cu-PTSM ($\log p = 1.95$) requires a nonaqueous solvent, ethanol or dimethylsulfoxide added to the labeling mixture with a level of 5%–10%,[34] which caused cell death (10% of initial cell population) during the cell-labeling procedure. The viability of ^{64}Cu-PTSM-labeled cells is not altered in the culture medium for 24 hours (Fig. 3A). The viability data are in close agreement with the previous report,[32] which showed that the toxic effects on the stem cell growth, viability, and differentiation were not observed at the same concentration of our study (10–20 μCi/mL of ^{64}Cu-PTSM). In our study, ^{64}Cu PTSM-labeled cells initially localized to the lungs and liver at 2 hours postinjection. Until 24 hours, the radioactivity in the lungs significantly decreased. In contrast with the radioactivity in the lungs, the radioactivity was mainly accumulated in the liver at 24 hours postinjection. The radioactivity in the liver may come from not only migrated K562-TL cells, but also effluxed ^{64}Cu. Following intravenously injection, released ionic copper is predominantly bound to the serum protein, albumin. When albumin is labeled with radiocopper, it transfers copper to hepatocytes.[10,35] Because the liver is a major organ of copper metabolism and clearance for ^{64}Cu-PTSM (Fig. 4), these cell-tracking results at 24 hours were not conclusive. Therefore, K562-TL cell trafficking at 24 hours needed further molecular biological studies to clarify these results.

BLI employs light-emitting proteins, known as luciferases, for real-time *in vivo* detection of migration and targeting of lymphocyte for cell therapy.[6] In our experiments, we used human chronic myelogenous leukemia cells retrovirally transduced firefly luciferase to confirm biodistribution of K562-TL cells. Due to low *in vivo* bioluminescent signals at 24 hours, we had to further analysis using *ex vivo* BLI. Semiquantitative data also showed significant reduction of bioluminescent signals in the lungs and slight increase of bioluminescent signals in the liver at 24 hours postcell injection (Fig. 7B). Since the light generation of luciferase regulated by the oxidation of D-luciferin in the presence of ATP and O_2, luminescence signals indicate K562-TL cells distribution in these organs. Distribution patterns of K562-TL cells were also confirmed by RT-PCR analysis of HSV1-tk mRNA (Fig. 8). RT-PCR results of tissue samples from the K562-TL cell-injected mouse indirectly demonstrate the existence of cells in the liver and clearance from the lungs at 24 hours. BLI and RT-PCR data confirmed the localization of K562-TL cells in the liver at 24 hours.

Direct cell-labeling methods have some limitations that dilution of radiotracers during cell division and the radiotracers released from the dead cells increase inaccuracy in image interpretation.[13] Indirect methods using HSV1-tk and *in vitro* FIAU labeling have a disadvantage that fast *in vivo* deiodination and efflux from labeled cells, but this strategy using *in vivo* FIAU labeling could be useful for serial and repetitive long-term tracking of cells with a proliferative potential by intravenous injection of short half-life ^{18}F-FIAU, because it showed specific uptake in HSV1-tk gene expressing tumor models.[36] Previous study[12] was able to image the migration of antigen-specific lymphocytes to targeting a tumor or an inflammatory site. However, K562-TL cells do not have a targeting ability to a specific site. Therefore, we would have to perform further experiments using immune or stem cells, which have the targeting ability to cancer or disease site.

Conclusions

The sensitivity of the reporter probe is an important consideration for cell-tracking studies. Our data show the advantages of ^{64}Cu-PTSM compared with ^{124}I-FIAU for the *in vivo* cell-trafficking study. The indirect-labeling method using HSV1-tk and FIAU showed high retention *in vitro*, but it displayed significantly fast clearance from labeled cells *in vivo*, including *in vivo* deiodination and physiological thyroid and stomach uptake. Even though ^{64}Cu-PTSM showed fast efflux from labeled cells *in vitro*, *in vivo* results described here support that ^{64}Cu-PTSM has good correlation with bioluminescence and RT-PCR analysis, and then the sufficient sensitivity to detect cells in early time point (~24 hours). The ^{64}Cu-PTSM-labeling method potentially could be translated into clinical practice to permit the noninvasive monitoring of cell therapies with immune cells or stem cells.

Acknowledgments

We appreciated the technical assistance about whole-body autoradiography from Kwang Sun Woo and Wee Sup Chung. This study was supported by a grant from the National R&D Program for Cancer Control, Ministry for Health, Welfare and Family affairs, Republic of Korea (0720420, 1120260) and National Research Foundation (NRF) and Ministry of Education, Science and Technology (MEST), Republic of Korea through its National Nuclear Technology Program (2011-0002291) and the Program of

Research and Development of Radiopharmaceuticals (50556-2011).

Disclosure Statement

There are no existing financial conflicts.

References

1. Akins EJ, Dubey P. Noninvasive imaging of cell-mediated therapy for treatment of cancer. J Nucl Med 2008;49 Suppl 2:180S.
2. Kiessling F. Noninvasive cell tracking. Handb Exp Pharmacol 2008;185 Pt 2:305.
3. Massoud TF, Gambhir SS. Molecular imaging in living subjects: Seeing fundamental biological processes in a new light. Genes Dev 2003;17:545.
4. Lewin M, Carlesso N, Tung CH, et al. Tat peptide-derivatized magnetic nanoparticles allow *in vivo* tracking and recovery of progenitor cells. Nat Biotechnol 2000;18:410.
5. Sutton EJ, Henning TD, Pichler BJ, et al. Cell tracking with optical imaging. Eur Radiol 2008;18:2021.
6. Dobrenkov K, Olszewska M, Likar Y, et al. Monitoring the efficacy of adoptively transferred prostate cancer-targeted human T lymphocytes with PET and bioluminescence imaging. J Nucl Med 2008;49:1162.
7. Edinger M, Cao YA, Verneris MR, et al. Revealing lymphoma growth and the efficacy of immune cell therapies using *in vivo* bioluminescence imaging. Blood 2003;101:640.
8. Edinger M, Hoffmann P, Contag CH, et al. Evaluation of effector cell fate and function by *in vivo* bioluminescence imaging. Methods 2003;31:172.
9. Hardy J, Edinger M, Bachmann MH, et al. Bioluminescence imaging of lymphocyte trafficking *in vivo*. Exp Hematol 2001;29:1353.
10. Adonai N, Nguyen KN, Walsh J, et al. *Ex vivo* cell labeling with ^{64}Cu-pyruvaldehyde-bis(N4-methylthiosemicarbazone) for imaging cell trafficking in mice with positron-emission tomography. Proc Natl Acad Sci U S A 2002;99:3030.
11. Li ZB, Chen K, Wu Z, et al. ^{64}Cu-labeled PEGylated polyethylenimine for cell trafficking and tumor imaging. Mol Imaging Biol 2009;11:415.
12. Koehne G, Doubrovin M, Doubrovina E, et al. Serial *in vivo* imaging of the targeted migration of human HSV-TK-transduced antigen-specific lymphocytes. Nat Biotechnol 2003;21:405.
13. Zanzonico P, Koehne G, Gallardo HF, et al. [^{131}I]FIAU labeling of genetically transduced, tumor-reactive lymphocytes: Cell-level dosimetry and dose-dependent toxicity. Eur J Nucl Med Mol Imaging 2006;33:988.
14. Ponomarev V. Nuclear imaging of cancer cell therapies. J Nucl Med 2009;50:1013.
15. Lucignani G, Ottobrini L, Martelli C, et al. Molecular imaging of cell-mediated cancer immunotherapy. Trends Biotechnol 2006;24:410.
16. Blocklet D, Toungouz M, Kiss R, et al. ^{111}In-oxine and ^{99m}Tc-HMPAO labelling of antigen-loaded dendritic cells: *In vivo* imaging and influence on motility and actin content. Eur J Nucl Med Mol Imaging 2003;30:440.
17. Nayak TK, Brechbiel MW. Radioimmunoimaging with longer-lived positron-emitting radionuclides: Potentials and challenges. Bioconjug Chem 2009;20:825.
18. Danos O, Mulligan RC. Safe and efficient generation of recombinant retroviruses with amphotropic and ecotropic host ranges. Proc Natl Acad Sci U S A 1988;85:6460.
19. Doubrovin M, Ponomarev V, Beresten T, et al. Imaging transcriptional regulation of p53-dependent genes with positron emission tomography *in vivo*. Proc Natl Acad Sci U S A 2001;98:9300.
20. Choi TH, Ahn SH, Kwon HC, et al. *In vivo* comparison of IVDU and IVFRU in HSV1-TK gene expressing tumor bearing rats. Appl Radiat Isot 2004;60:15.
21. Kim JY, Park H, Lee JC, et al. A simple Cu-64 production and its application of Cu-64 ATSM. Appl Radiat Isot 2009; 67:1190.
22. Woo SK, Lee TS, Kim KM, et al. Anesthesia condition for ^{18}F-FDG imaging of lung metastasis tumors using small-animal PET. Nucl Med Biol 2008;35:143.
23. Gambhir SS, Barrio JR, Wu L, et al. Imaging of adenoviral-directed herpes simplex virus type 1 thymidine kinase reporter gene expression in mice with radiolabeled ganciclovir. J Nucl Med 1998;39:2003.
24. Laemmli UK. Cleavage of structural proteins during the assembly of the head of bacteriophage T4. Nature 1970;227:680.
25. Tjuvajev JG, Avril N, Oku T, et al. Imaging herpes virus thymidine kinase gene transfer and expression by positron emission tomography. Cancer Res 1998;58:4333.
26. Tjuvajev JG, Finn R, Watanabe K, et al. Noninvasive imaging of herpes virus thymidine kinase gene transfer and expression: A potential method for monitoring clinical gene therapy. Cancer Res 1996;56:4087.
27. Brust P, Haubner R, Friedrich A, et al. Comparison of [^{18}F]FHPG and [$^{124/125}$I]FIAU for imaging herpes simplex virus type 1 thymidine kinase gene expression. Eur J Nucl Med 2001;28:721.
28. Haubner R, Avril N, Hantzopoulos PA, et al. *In vivo* imaging of herpes simplex virus type 1 thymidine kinase gene expression: Early kinetics of radiolabelled FIAU. Eur J Nucl Med 2000;27:283.
29. Shields AF, Grierson JR, Kozawa SM, et al. Development of labeled thymidine analogs for imaging tumor proliferation. Nucl Med Biol 1996;23:17.
30. Chou TC, Feinberg A, Grant AJ, et al. Pharmacological disposition and metabolic fate of 2′-fluoro-5-iodo-1-beta-D-arabinofuranosylcytosine in mice and rats. Cancer Res 1981;41:3336.
31. Tjuvajev JG, Doubrovin M, Akhurst T, et al. Comparison of radiolabeled nucleoside probes (FIAU, FHBG, and FHPG) for PET imaging of HSV1-tk gene expression. J Nucl Med 2002;43:1072.
32. Bennink RJ, Thurlings RM, van Hemert FJ, et al. Biodistribution and radiation dosimetry of ^{99m}Tc-HMPAO-labeled monocytes in patients with rheumatoid arthritis. J Nucl Med 2008;49:1380.
33. Botti C, Negri DR, Seregni E, et al. Comparison of three different methods for radiolabelling human activated T lymphocytes. Eur J Nucl Med 1997;24:497.
34. Huang J, Lee CC, Sutcliffe JL, et al. Radiolabeling rhesus monkey CD34+ hematopoietic and mesenchymal stem cells with ^{64}Cu-pyruvaldehyde-bis(N4-methylthiosemicarbazone) for microPET imaging. Mol Imaging 2008;7:1.
35. Blower PJ, Lewis JS, Zweit J. Copper radionuclides and radiopharmaceuticals in nuclear medicine. Nucl Med Biol 1996;23:957.
36. Alauddin MM, Shahinian A, Park R, et al. *In vivo* evaluation of 2′-deoxy-2′-[^{18}F]fluoro-5-iodo-1-beta-D-arabinofuranosyluracil ([^{18}F]FIAU) and 2′-deoxy-2′-[^{18}F]fluoro-5-ethyl-1-beta-D-arabinofuranosyl uracil ([^{18}F]FEAU) as markers for suicide gene expression. Eur J Nucl Med Mol Imaging 2007;34:822.